A Semiclassical Simulation of Raman Scattering with Ehrenfest+R Dynamics

Hsing-Ta Chen,[1, a)] Tao E. Li,[1] Maxim Sukharev,[2, 3] Abraham Nitzan,[1] and Joseph E. Subotnik[1]
[1)] *Department of Chemistry, University of Pennsylvania, Philadelphia, Pennsylvania 19104, U.S.A.*
[2)] *Department of Physics, Arizona State University, Tempe, Arizona 85287, USA*
[3)] *College of Integrative Sciences and Arts, Arizona State University, Mesa, AZ 85212, USA*

We generalize the recently proposed Ehrenfest+R algorithm [J. Chem. Phys.] to explore Raman scattering. While the usual Ehrenfest mixed quantum-classical framework propagates both a quantum subsystem (with the Schrödinger equation) and the classical electromagnetic fields (with Maxwell's equations) self-consistently, Ehrenfest+R dynamics goes further by including an additional emprirical relaxation to recover the correct spontaneous emission rate. As a result of this correction, we show here that Ehrenfest+R dynamics recover qualitatively significant features that are absent from standard Ehrenfest dynamics, including both resonant and off-resonant Raman signals. For resonant Raman scattering, Ehrenfest+R dynamics are in quantitative agreement with Kramers-Heisenberg-Dirac (KHD) theory.

I. INTRODUCTION

Recently there has been an explosion of interest in Raman scattering, especially surface- and tip-enhanced Raman scattering[1–6], as a probe to investigate plasmonic excitations of molecules near a metal surface[7,8] and chemical reactions at catalytic surfaces.[9] In general, the Raman technique offers the experimentalist detailed information about how the vibrations couple to charges in electronic polarization, and is very relevant for modern experiments with metallic nanoclusters. Furthermore, Raman spectroscopy also has the additional advantage of offering clean signals in aqueous medium where water IR bands can obscure signals.

From a quantitative point of view, the current theory of molecular Raman scattering is based on the Kramers-Heisenberg-Dirac (KHD) formalism[10,11] which can be reduced to Placzek's classical theory of polarizability for off-resonance cases[12,13], as well as Albrecht's vibronic theory for resonant Raman scattering.[14–16] Over the years, efficient semiclassical tools have been developed to evaluate Raman spectra approximately within the KHD formalsim using an excited-state gradient approximation to propagate short time dynamics.[13,17–20] More recently, chemists have also incorporated electronic structure theories into the semiclassical description of Raman spectroscopy.[21–24] In general, because it relies on a sum over all states (nuclear and electronic), the KHD formalism can be difficult to implement in practice.

One long term goal for our research groups is to study plasmonic systems with strong light-matter couplings where Raman scattering is a very sensitive probe of the collective behavior of electronic dynamics.[25] For such systems, a direct implementation of KHD theory is not feasible (because of the large number of states required) and is also likely not relevant (because the presence of strong light-matter should invalidate perturbation theory). Thus, in order for us to model such systems, and to take into account strong light-matter couplings, the most natural approach is to consider the quantum subsystems and classical electromagnetic (EM) fields on an equal footing. This approach stands in contrast to most existing semiclassical approaches for spectroscopy, which treat the incoming field as an fixed external perturbation, and extrapolate the behavior of quantum subsystems to predict light emission.[20,26,27]

Now, obviously, any computational approach to spectroscopy that promises "equal footing" for light and matter will necessarily require large approximations; in particular, we expect that a quantum treatment of the EM field will be prohibitively difficult, and one will necessarily need to work with classical electromagnetic fields. The simplest example of such a mixed quantum-classical approach is self-consistent Ehrenfest dynamics. Unfortunately, Ehrenfest dynamics do not fully recover spontaneous emission and thus are unlikely to capture Raman scattering either.[28] That being said, we are unaware of a systematic study answering this question.

Now, very recently, our laboratory has proposed an improved so-called "Ehrenfest+R" algorithm that builds in spontaneous emission on top of Ehrenfest dynamics by enforcing additional relaxation for two-level systems.[29] If this "+R" approach can be generalized beyond two-level systems, the resulting improved mean-field dynamics should have the potential to capture Raman scattering and open up new avenues for studying light-matter interactions within

[a)] Electronic mail: hsingc@sas.upenn.edu

a mixed quantum-classical theory framework. Thus, in this communication, our goal is generalize Ehrenfest+R to the case of a multi-level (i.e. more than two-level) quantum subsystem. Furthermore, we will show that such a generalization can indeed capture both resonant and off-resonant Raman scattering (at least for a three-level molecular system); Our results is in quantitative agreement with KHD theory. The data presented here strongly suggests that Ehrenfest+R dynamics (and other spruced-up versions of mean-field dynamics) can be excellent tools for exploring interesting light-matter interactions far beyond basic absorption of Raman theory at the level of KHD formalism (and applicable to large subsystems, e.g., plasmonic systems).

This communication is organized as follows. In Sec. II, we review the KHD formalism and calculate the polarizability and Raman scattering profile for a three-level system. In Sec. III, we formulate an Ehrenfest+R approach for a three-level system. In Sec. IV, we show Ehrenfest+R dynamics results for Raman spectra and compare against the KHD formalism. In Sec. V, we conclude. In this communication, we use a bold symbol to denote a space vector in Cartesian coordinate, such as $\mathbf{E}(\mathbf{r}) = E_x(\mathbf{r})\,\hat{\mathbf{x}} + E_y(\mathbf{r})\,\hat{\mathbf{y}} + E_z(\mathbf{r})\,\hat{\mathbf{z}}$, and $\widehat{H}$ denotes a quantum operator. We work in SI units.

II. QUANTUM THEORY OF RAMAN SCATTERING

Raman light scattering is an inelastic process whereby the interaction between the incident photons and molecules can lead to an energy shift in emission spectra for a small fraction of the scattered photons. To qualitatively describe Raman light scattering, consider a molecular system with interactions between electronic states and nuclear vibrations. Incident photons excite the molecular system to an intermediate state (which could be a virtual state), and that intermediate state is subsequently coupled both to the ground state as well to other vibronic states. Thus, the system can emit photons with two different frequencies through spontaneous emission.[30] On the one hand, a transition back to the ground state yields scattered photons with the same energy with the incident photons (which is known as Rayleigh scattering). On the other hand, a transition to other vibronic states will generate scattered photons with energies different from the incident photons (which is known as Raman scattering).

In this section, we review the KHD dispersion formula which quantifies the Raman scattering cross section[10,14,31] assuming knowledge of the polarizability; we evaluate the KHD formalism for a three-level model system in 1D space.

A. Kramers-Heisenberg-Dirac Formalism

For a quantitative description of Raman scattering, the KHD formula is the standard, frequency domain expression for the scattering cross section[13]

$$\sigma_{fi}^{\mathrm{3D}}(\omega_S, \omega_I) = \frac{8\pi\omega_I\omega_S^3}{9c^4}\sum_{\rho,\lambda}\left|\left[\alpha_{fi}(\omega_I)\right]^{\nu\nu'}\right|^2, \tag{1}$$

where the polarizability is given by

$$\begin{aligned}\left[\alpha_{fi}(\omega_I)\right]^{\nu\nu'} = -\sum_{k,n}\Bigg(&\frac{\langle\psi_f|\,\widehat{\mu}^{\nu}\,|\psi_{k,n}\rangle\,\langle\psi_{k,n}|\,\widehat{\mu}^{\nu'}\,|\psi_i\rangle}{\varepsilon_i + \hbar\omega_I - \varepsilon_{kn} + i\hbar\gamma}\\ &+\frac{\langle\psi_f|\,\widehat{\mu}^{\nu'}\,|\psi_{k,n}\rangle\,\langle\psi_n|\,\widehat{\mu}^{\nu}\,|\psi_i\rangle}{\varepsilon_f - \hbar\omega_I - \varepsilon_{kn} + i\hbar\gamma}\Bigg),\end{aligned} \tag{2}$$

The frequency of the incident photons is ω_I and the frequency of the scattered photons is ω_S; these frequencies satisfy energy conservation $\hbar\omega_S = \varepsilon_i + \hbar\omega_I - \varepsilon_f$. The KHD formula is known as the "sum-over-states" formula since the polarizability expression requires a summation over all possible intermediate states $\psi_{k,n}$ where the index k labels electronic states and the index n labels vibrational states corresponding to electronic states. $\widehat{\mu}^{\nu}$ denotes the transition dipole moment operator for $\nu = \{x, y, z\}$. The linewidth γ corresponds to the average lifetime of the intermediate state.

According to the scattering cross section given by Eq. (1), Raman spectroscopy is a two-photon spectroscopy. Experimentaly, one typically fixes ω_I and observes the emission spectrum as a function of ω_S. The frequency $\omega_S = \omega_I$ corresponds to the contribution of Rayleigh scattering, and other emission peaks are attributed to Raman scattering. The KHD formula is derived using second order perturbation theory for a quantum subsystem in the presence of the incident photons[13], and the scattering cross section is extrapolated from the change in electronic population.

B. Three-level System

To quantify the KHD Raman scattering formalism, we consider a model system with three vibronic states: two lower energy states for an electronic ground state with different vibrational modes: $|gn_1\rangle \equiv |0\rangle$ and $|gn_1'\rangle \equiv |1\rangle$ and one for an excited state $|en_2\rangle \equiv |2\rangle$. We assume the energies of the vibronic states are $\varepsilon_0 \leq \varepsilon_1 < \varepsilon_2$ and the electric dipole interactions couple the ground and excited states only. Thus, the electronic Hamiltonian is given by

$$\widehat{H}^{\mathrm{el}} = \begin{pmatrix} \varepsilon_0 & 0 & \mathcal{V}_{02} \\ 0 & \varepsilon_1 & \mathcal{V}_{12} \\ \mathcal{V}_{02}^* & \mathcal{V}_{12}^* & \varepsilon_2 \end{pmatrix} \tag{3}$$

where the electric dipole coupling is

$$\mathcal{V}_{ij} = -\int \mathrm{d}x \mathbf{E}\left(x,t\right) \cdot \boldsymbol{\mathcal{P}}_{ij}\left(x\right). \tag{4}$$

in a 1D space.

For frequency domain measurement, consider a single-mode incoming continuous wave (CW) electromagnetic field with frequency ω_I,

$$\mathbf{E}_I\left(x,t\right) = \frac{A_I}{\sqrt{\epsilon_0}} \cos\left(k_I x - \omega_I t\right) \hat{\mathbf{z}} \tag{5}$$

$$\mathbf{B}_I\left(x,t\right) = -\sqrt{\mu_0} A_I \sin\left(k_I x - \omega_I t\right) \hat{\mathbf{y}} \tag{6}$$

where $\omega_I = ck_I$ and A_I is the amplitude of the incoming field. We assume the spatial size of the polarization is small in space, i.e. $\boldsymbol{\mathcal{P}}_{ij}\left(x\right) \approx \mu_{ij}\delta\left(x\right)\hat{\mathbf{z}}$, so that the electric dipole interactions are approximated as $\int \mathrm{d}x \mathbf{E}\left(x,t\right) \cdot \boldsymbol{\mathcal{P}}_{ij}\left(x\right) \approx \mu_{ij}\frac{A_I}{\sqrt{\epsilon_0}}\cos\left(\omega_I t\right)$.

For light scattering in a 1D space, the scattering cross section is defined as the ratio between the number of photons scattered per time divided by the number of photons incident per time. With this definition, the KHD Raman cross section becomes in 1D (see Appendix A):

$$\sigma_{fi}^{\mathrm{1D}}\left(\omega_S, \omega_I\right) = \frac{\omega_I \omega_S}{2c^2} \left|\alpha_{fi}^{\mathrm{1D}}\left(\omega_I\right)\right|^2 \tag{7}$$

For a three-level system, the KHD expression for the polarizability is

$$\begin{aligned} \alpha_{fi}^{\mathrm{1D}}\left(\omega_I\right) = -\Bigg(& \frac{\mu_{02}\mu_{12}}{\varepsilon_i + \hbar\omega_I - \varepsilon_2 + i\hbar\gamma} \\ & + \frac{\mu_{02}\mu_{12}}{\varepsilon_f - \hbar\omega_I - \varepsilon_2 + i\hbar\gamma} \Bigg). \end{aligned} \tag{8}$$

Here we take linewidth γ to be the average lifetime for the electronic transitions of the excited state:

$$\frac{1}{\gamma} = \frac{1}{2}\left(\frac{1}{\kappa_{02}} + \frac{1}{\kappa_{12}}\right), \tag{9}$$

where the corresponding Fermi's golden rule (FGR) rates are given by

$$\kappa_{fi} = \frac{\varepsilon_i - \varepsilon_f}{\hbar^2 \epsilon_0 c} \mu_{fi}^2. \tag{10}$$

In the case of resonant Stokes or anti-Stokes Raman scattering (where the incident photon lines up with the excited state, i.e. $\varepsilon_i + \hbar\omega_I = \varepsilon_2$), the first term in Eq. (8) dominates. Resonant Raman scattering signals are composed of two signals: (i) When $\hbar\omega_I = \varepsilon_2 - \varepsilon_0$ and the scattered photon energy is $\hbar\omega_S = \varepsilon_2 - \varepsilon_1$, the polarizability term with $i = 0$ and $f = 1$ ($\alpha_{10}^{\mathrm{1D}}\left(\omega_I\right)$) leads to a Stokes Raman peak (i.e. $\omega_S < \omega_I$). (ii) When $\hbar\omega_I = \varepsilon_2 - \varepsilon_1$ the scattered photon energy is $\hbar\omega_S = \varepsilon_2 - \varepsilon_0$, the polarizability term with $i = 1$ and $f = 0$ ($\alpha_{01}^{\mathrm{1D}}\left(\omega_I\right)$) leads to an anti-Stokes Raman peak (i.e. $\omega_S > \omega_I$). Obviously, anti-Stokes Raman scattering can occur only state $|1\rangle$ is occupied at steady state.

In the case that the incident photon does not line up with any excited state, the excitation is detuned far off resonance (known as off-resonance Raman scattering). In this case, the intermediate state of the light scattering process is a visual state, i.e. $\varepsilon_k = \varepsilon_i + \hbar\omega_I$, and the two terms in Eq. (8) both contribute meaningfully to the Raman cross section. Of course, for a weak field, scattered photons are always dominated by Rayleigh scattering (i.e. $\omega_S = \omega_I$).

III. EHRENFEST+R APPROACH FOR RAMAN SCATTERING

Given that Raman scattering is based on spontaneous emission,[30] Ehrenfest+R dynamics should provide a proper tool for a mixed quantum-classical simulation since the algorithm was designed to recover spontaneous emission. One can generalize the Ehrenfest+R method to the case of more than a two level system as follows: we add distinct +R corrections for electronic transitions between individual pairs of vibronic states, i.e. $2 \to 0$ and $2 \to 1$. Furthermore, to reach steady state, we allow a phenomenological, non-radiative dissipation between $|0\rangle$ and $|1\rangle$. In this section, we start by formulating such a generalized Ehrenfest+R approach in the context of the three-level system; thereafter we compare Ehrenfest+R results against the KHD formula.

A. Generalized Ehrenfest+R Method

For the Hamiltonian given by Eq. (3), there are two electronic transitions that are mediated electric dipole couplings $\mathcal{V}_{02}$ and $\mathcal{V}_{12}$ which corresponds to spontaneous emission rates κ_{02} and κ_{12} given by Eq. (10). Here, based on Ref. 29, we will add two pairwise +R corrections on top of Ehrenfest dynamics in order to recover the individual spontaneous emission rates (κ_{fi}) from $|i\rangle$ to $|f\rangle$ while keeping the other state populations fixed.

1. System propagator

To implement a pairwise treatment for Ehrenfest+R dynamics, the Liouville equation (together with additional relaxations) can be written as

$$\frac{\partial \widehat{\rho}}{\partial t} = -\frac{i}{\hbar}\left[\widehat{H}^{\mathrm{el}}, \widehat{\rho}\right] + \mathcal{L}_R^{2\to 0}\widehat{\rho} + \mathcal{L}_R^{2\to 1}\widehat{\rho}, \tag{11}$$

Here, the diagonal elements of the $\mathcal{L}_R^{i\to f}$ super-operators are defined by

$$\left[\mathcal{L}_R\widehat{\rho}\right]_{ii} = -\left[\mathcal{L}_R\widehat{\rho}\right]_{ff} = -k_R^{fi}\rho_{ii}, \tag{12}$$

and the off-diagonal element of $\left[\mathcal{L}_R\widehat{\rho}\right]_{ij}$ are chosen to maintain the purity of the density matrix $\left[\mathcal{L}_R^{i\to f}\widehat{\rho}\right]$. The +R relaxation rate k_R^{fi} for the transistion $i \to f$ is given by

$$k_R^{fi} \equiv 2\kappa_{fi}\left(1-\rho_{ff}\right)\mathrm{Im}\left[\frac{\rho_{fi}}{|\rho_{fi}|}e^{i\phi}\right]^2. \tag{13}$$

$\phi \in (0, 2\pi)$ is a phase chosen randomly for each Ehrenfest+R trajectory.

In practice, we use a pure state representation for the density matrix: $\widehat{\rho} = |\psi\rangle\langle\psi|$ with wavefunction $|\psi(t)\rangle = c_0(t)|0\rangle + c_1(t)|1\rangle + c_2(t)|2\rangle$. The additional relaxation embodied by $\mathcal{L}_R^{i\to f}$ is defined by a transition operator:

$$\mathcal{T}\left[k_R^{fi}\right]: \begin{pmatrix} \vdots \\ c_i \\ \vdots \\ c_f \\ \vdots \end{pmatrix} \to \begin{pmatrix} \vdots \\ \frac{c_i}{|c_i|}\sqrt{|c_i|^2 - k_R^{fi}|c_i|^2\,dt} \\ \vdots \\ \frac{c_f}{|c_f|}\sqrt{|c_f|^2 + k_R^{fi}|c_f|^2\,dt} \\ \vdots \end{pmatrix}. \tag{14}$$

Thus in practice, the time evolution of the subsystem wavefunction is carried out by

$$|\psi(t+dt)\rangle = \mathcal{T}\left[k_R^{12}\right]\mathcal{T}\left[k_R^{02}\right]e^{-i\widehat{H}^{\mathrm{el}}dt/\hbar}|\psi(t)\rangle. \tag{15}$$

where $e^{-i\widehat{H}^{\mathrm{el}}dt/\hbar}$ is responsible for propagating according to the first term of Eq. (11). Note that $\mathcal{T}\left[k_R^{12}\right]$ and $\mathcal{T}\left[k_R^{02}\right]$ commute as long as dt is sufficiently small.

2. EM field propagator

We write the total EM field in the form of $\mathbf{E} = \mathbf{E}_I + \mathbf{E}_S$ and $\mathbf{B} = \mathbf{B}_I + \mathbf{B}_S$ where $\mathbf{E}_S$ and $\mathbf{B}_S$ are the scattered EM fields. For a CW field given by Eq. (5) and Eq. (6), $\mathbf{E}_I$ and $\mathbf{B}_I$ satisfy source-less Maxwell's equations, so we can treat the CW field as a standalone external field. Therefore, for underlying Ehrenfest dynamics, the scattered fields $\mathbf{E}_S$ and $\mathbf{B}_S$ satisfy Maxwell's equations:

$$\frac{\partial}{\partial t}\mathbf{B}_S = -\boldsymbol{\nabla} \times \mathbf{E}_S, \tag{16}$$

$$\frac{\partial}{\partial t}\mathbf{E}_S = c^2 \boldsymbol{\nabla} \times \mathbf{B}_S - \frac{1}{\epsilon_0}\mathbf{J}, \tag{17}$$

where the average current is

$$\mathbf{J}(x,t) = \sum_{i=2}\sum_{f=0,1} 2\left(\varepsilon_f - \varepsilon_i\right) \mathrm{Im}\left[\rho_{fi}(t)\right] \boldsymbol{\mathcal{P}}_{fi}(x). \tag{18}$$

Given the pairwise transitions of the subsystem, the classical EM field must be rescaled. We denote the rescaling operator for the EM fields by:

$$\mathcal{R}\left[\delta U_R^{fi}\right] : \begin{pmatrix} \mathbf{E}_S \\ \mathbf{B}_S \end{pmatrix} \to \begin{pmatrix} \mathbf{E}_S + \alpha^{fi}\delta\mathbf{E}_R^{fi} \\ \mathbf{B}_S + \beta^{fi}\delta\mathbf{B}_R^{fi} \end{pmatrix}. \tag{19}$$

where the rescaling coefficients are chosen to be

$$\alpha^{fi} = \sqrt{\frac{cdt}{\Lambda^{fi}} \frac{\delta U_R^{fi}}{\epsilon_0 \int \mathrm{d}v \left|\delta\mathbf{E}_R^{fi}\right|^2}} \times \mathrm{sgn}\left(\mathrm{Im}\left[\rho_{fi} e^{i\phi}\right]\right), \tag{20}$$

$$\beta^{fi} = \sqrt{\frac{cdt}{\Lambda^{fi}} \frac{\mu_0 \delta U_R^{fi}}{\int \mathrm{d}v \left|\delta\mathbf{B}_R^{fi}\right|^2}} \times \mathrm{sgn}\left(\mathrm{Im}\left[\rho_{fi} e^{i\phi}\right]\right). \tag{21}$$

Here Λ^{fi} is the self-interference length (see Ref. 29). For a Gaussian polarization profile (as in Eq. (27)) $\Lambda^{fi} = 2.363/\sqrt{2a}$. The energy change for each pairwise relaxation $i \to f$ is

$$\delta U_R^{fi} = \left(\varepsilon_i - \varepsilon_f\right) k_R^{fi} \rho_{ii} dt. \tag{22}$$

According to Eq. (15), we need to perform two rescaling operators ($\mathcal{R}\left[\delta U_R^{12}\right]$ and $\mathcal{R}\left[\delta U_R^{02}\right]$) corresponding to the two relaxation pathways ($2 \to 0$ and $2 \to 1$).

For the results below, we assume without loss of generality that the transition dipole moments are the same for both the $2 \to 1$ and $2 \to 0$ transitions, i.e.$\boldsymbol{\mathcal{P}}_{02} = \boldsymbol{\mathcal{P}}_{12} = \boldsymbol{\mathcal{P}}$, so that the rescaling fields can be chosen to be $\delta\mathbf{E}_R^{fi} = \delta\mathbf{E}_R$ and $\delta\mathbf{B}_R^{fi} = \delta\mathbf{B}_R$. For a 1D system, the rescaling fields take the form

$$\delta\mathbf{E}_R = \boldsymbol{\nabla} \times \boldsymbol{\nabla} \times \boldsymbol{\mathcal{P}} - g\boldsymbol{\mathcal{P}}, \tag{23}$$

$$\delta\mathbf{B}_R = -\boldsymbol{\nabla} \times \boldsymbol{\mathcal{P}} - h\left(\boldsymbol{\nabla}\times\right)^3 \boldsymbol{\mathcal{P}}, \tag{24}$$

As demonstrated in Ref. 29, for Gaussian polarization, we choose $g = 2a$ and $h = 1/6a$. With this assumption, we can combine the two rescaling operators as $\mathcal{R}\left[\delta U_R^{12} + \delta U_R^{02}\right]$.

In the end, each Ehrenfest+R trajectory for classical EM fields is propagated by

$$\begin{pmatrix} \mathbf{E}_S(t+dt) \\ \mathbf{B}_S(t+dt) \end{pmatrix} = \mathcal{R}\left[\delta U_R^{12} + \delta U_R^{02}\right] \mathcal{M}[dt] \begin{pmatrix} \mathbf{E}_S(t) \\ \mathbf{B}_S(t) \end{pmatrix}. \tag{25}$$

Here $\mathcal{M}[dt]$ denotes the linear propagator of Maxwell's equations (Eq. (16) and (17)) for time step dt.

3. Non-radiative dissipation

Without any dissipation allowed for, the three-level system Eq. (3) eventually reaches the asymptotic state, $|\psi(t\to\infty)\rangle = |1\rangle$, in the presence of the CW field. By contrast, to reach the correct steady state, we must take into account vibrational relaxation. Thus, we also introduce a phenomenological, non-radiative relaxation from $|1\rangle$ to $|0\rangle$ by a transition operator:

$$|\psi(t+dt)\rangle \to \mathcal{T}\left[k_{\rm vib}^{01}\right]|\psi(t+dt)\rangle\,. \tag{26}$$

where the operation of the transition operator $\mathcal{T}$ is defined in Eq. (14). The classical EM field is not rescaled for this non-radiative transition, and the vibrational decay rate $k_{\rm vib}^{01}$ is an empirical parameter which will to be specified later. Note that we exclude thermal transitions from $|0\rangle$ to $|1\rangle$ since we assume the system is at small enough temperature.

In the end, Ehrenfest+R dynamics are specified by Eqs. (15), (25), and (26).

IV. RESULTS

A. Parameters

As far as simulating Raman scattering by Ehrenfest+R approach, we consider a three-level system with $\varepsilon_0 = 0$, $\varepsilon_1 = \frac{1}{4}\hbar\Omega = 4.115$ eV, and $\varepsilon_2 = \hbar\Omega = 16.46$ eV. We assume the initial state of the system is the ground state, $|\psi(t=0)\rangle = |0\rangle$ and we turn on the incident CW field at $t = 0$. The transition dipole moment takes the form of a Gaussian distribution:

$$\boldsymbol{\mathcal{P}}_{02}(x) = \boldsymbol{\mathcal{P}}_{12}(x) = \mu\sqrt{\frac{a}{\pi}}e^{-ax^2}\hat{\mathbf{z}}, \tag{27}$$

where $\mu = 11282$ C/nm/mol and $a = 1/2\sigma^2$ with $\sigma = 3.0$ nm. With this polarization, the rescaling fields are (from Ref. 29):

$$\delta\mathbf{E}_R(x) = -\mu\sqrt{\frac{a}{\pi}}4a^2x^2e^{-ax^2}\hat{\mathbf{z}}, \tag{28}$$

$$\delta\mathbf{B}_R(x) = \mu\sqrt{\frac{a}{\pi}}\frac{4}{3}a^2x^3e^{-ax^2}\hat{\mathbf{y}}. \tag{29}$$

We run dynamics for 500 fs to reach a steady state, averaging over $N_{\rm traj} = 50$ trajectories.

1. Resonance and off-resonance scatterings

We first focus on Raman scattering in the frequency-domain spectrum. In Fig. 1, we plot the Fourier transform of the scattered electric field ($\mathbf{E}_S$) at steady state as a function of ω_S for various incident frequencies ω_I. When the incident field is far from resonance, we find that the scattered EM field is dominated by Rayleigh scattering ($\omega_S = \omega_I$), as expected from the KHD formula. Qualitatively, both standard Ehrenfest dynamics and Ehrenfest+R dynamics predict Rayleigh scattering peaks at the correct frequency and show a linear shift with respect to the incident frequency.

When the incident photon is at resonance (i.e. the incident frequency ω_I lines up with electronic excitation), Ehrenfest+R dynamics captures Raman scattering peaks qualitatively, and we observe two resonance scattering outcomes at steady state: Stokes Raman scattering peak at $(\omega_I, \omega_S) = \left(\Omega, \frac{3}{4}\Omega\right)$ and anti-Stokes Raman scattering peak at $(\omega_I, \omega_S) = \left(\frac{3}{4}\Omega, \Omega\right)$. The Stokes Raman scattering occurs when the incident frequency is $\omega_I = \varepsilon_2 - \varepsilon_0$ and the anti-Stokes Raman scattering occurs when $\omega_I = \varepsilon_2 - \varepsilon_1$. In general, the anti-Stokes peak is far smaller than the Stokes peak. In fact, we re-emphasize that, for an anti-Stokes peak, we must have population present on state $|1\rangle$ at steady state. To probe this feature, we can adjust the vibrational decay rate $k_{\rm vib}^{01}$. In the left panel of Fig. 1, the vibrational decay rate ($k_{\rm vib}^{01}$) is large so that population of state $|1\rangle$ relax to state $|0\rangle$ fast, and thus the anti-Stokes peak at $(\omega_I, \omega_S) = \left(\frac{3}{4}\Omega, \Omega\right)$ is small. In the right panel of Fig. 1, we decrease the vibrational decay rate ($k_{\rm vib}^{01}$) so that the population of state $|1\rangle$ lingers longer, and therefore an anti-Stokes Raman peak emerges.

In contrast to Ehrenfest+R dynamics, in Fig. 1 we also plot the spectra obtained from standard Ehrenfest calculations. Ehrenfest dynamics capture only Rayleigh scattering peaks and not Raman scattering peaks. To rationalize

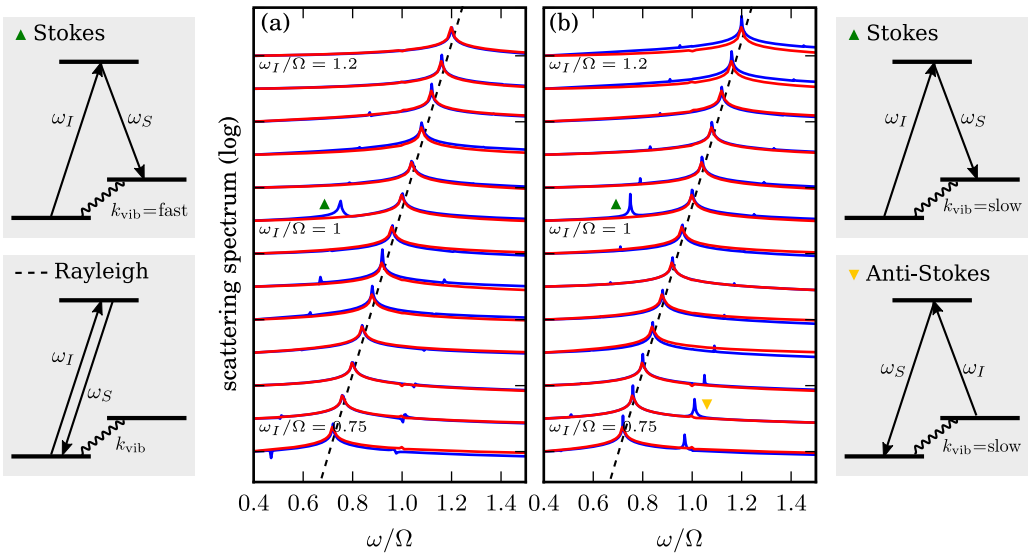

Figure 1. Raman spectra as a function of ω_S/Ω when varying the incident CW field frequency ω_I/Ω. Standard Ehrenfest dynamics are colored red, and Ehrenfest+R dynamics are colored blue. For visualization purposes, the spectrum is plotted in log-scale. The incoming field amplitude is $A_I/\sqrt{\hbar\Omega} = 10^{-2}$. We choose vibrational decay rates to be (a) fast $k_{\rm vib}^{01} = 1$ [1/fs] and (b) slow $k_{\rm vib}^{01} = 0.1$ [1/fs]. For all CW frequencies, Rayleigh scattering peaks are observed at $\omega_S = \omega_I$ (central peak). The Stokes resonance Raman scattering occurs at $\omega_S/\Omega = 0.75$ when $\omega_I/\Omega = 1$; the anti-Stokes resonant Raman scattering occurs at $\omega_S/\Omega = 1$ when $\omega_I/\Omega = 0.75$. For strong dissipation (panel (a)), the anti-Stokes resonance Raman is suppressed. Note that Ehrenfest+R dynamics can recover both resonant Raman scattering peaks while standard Ehrenfest dynamics does not predict any Raman scattering.

this behavior, we recall that the Ehrenfest decay rate for spontaneous emission depends linearly on the lower state population.[29] For the initial state $c_0 = 1$ and $c_1 = c_2 = 0$, the system is excited to state $|2\rangle$ by the incident field, but will never populate state $|1\rangle$. Therefore, effectively we always have $c_1 = 0$ within Ehrenfest dynamics and the spontaneous emission via electronic transition $2 \to 1$ never occurs. As a general rule of thumb, because standard Ehrenfest dynamics are effectively classical dynamics, whereas there is only a single frequency ω_I in the EM field and the EM field strength is weak, Ehrenfest dynamics will predict all response to be at the same frequency ω_I.

2. *Resonant Raman scattering*

We now turn our attention to the near-resonant regime, i.e. $\omega_I \approx \Omega$, and focus on Stokes Raman scattering. To compare against the KHD formula, we extract the scattering cross section from Ehrenfest+R dynamics by

$$\sigma_{10}^{\rm 1D}(\omega_S, \omega_I) = \frac{|\mathbf{E}_S(\omega_S)|^2/\omega_S}{A_I^2/\omega_I}, \tag{30}$$

according to the definition of 1D scattering cross section and Einstein relation (see Eq. A5). Here we denote the intensity of the Raman scattering signal at frequency ω_S as $|\mathbf{E}_S(\omega_S)|^2$ where $\mathbf{E}_S(\omega_S)$ is the amplitude of the scattered field satisfying $\mathbf{E}_S(x,t) = \sum_{\omega_S} \mathbf{E}_S(\omega_S)\cos(k_S x - \omega_S t)$.

In Fig. 2(a), we compare Ehrenfest+R dynamics with the KHD formula (Eq. (7)). We demonstrate that Ehrenfest+R dynamics can quantitatively recover the enhancement of the Raman scattering cross section in the nearly resonant regime, while the standard Ehrenfest dynamics does not predict any enhancement. Furthermore, the linewidth obtained by Ehrenfest+R approach agrees with the average lifetime for the KHD formula (Eq. (9)). In Fig. 2(b), the difference between standard Ehrenfest and Ehrenfest+R results are plotted in logarithmic scale. The +R correction is necessary in order for semiclassical simulations to recover resonance Raman scattering.

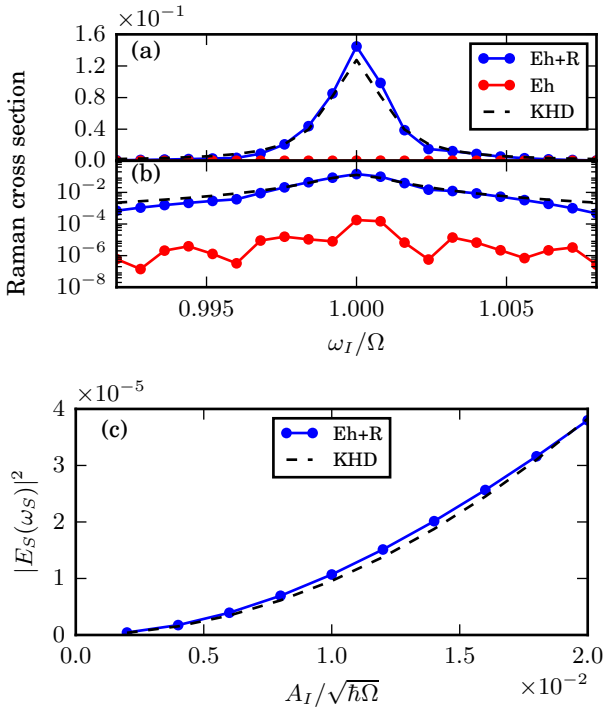

Figure 2. (a,b) Raman scattering cross section as a function of incident frequency near resonance ($\omega_I/\Omega \approx 1$). Standard Ehrenfest dynamics are colored red, and Ehrenfest+R dynamics are colored blue. The KHD formula is plotted in dashed line. The incoming field amplitude is $A_I/\sqrt{\hbar\Omega} = 10^{-2}$. (a) is a linear plot and (b) is a semi-log plot. In panel (c), resonant Raman scattering signal intensity is plotted as a function of incident CW amplitude A_I. The incident and scattered frequencies are $\omega_I = \Omega$ and $\omega_S = 0.75\Omega$. The black dashed line is the intensity given by the KHD formula (Eq. (31)). Note that both KHD and Ehrenfest+R are capturing Raman signals that are linear with respect to the incoming filed. For the non-radiative dissipation, we choose a vibrational decay rate $k^{01}_{\text{vib}} = 0.1$ [1/fs].

3. *Field strength*

Finally we focus on the intensity of resonance Raman scattering (i.e. $\omega_I = \Omega$) in response to various incident field amplitudes. Indeed, one might question whether or not the Raman signals as predicted by Ehrefenst+R dynamics scale correctly with respect to the EM field strength; indeed a devil's advocate might argue that these "Raman-like" feature emerging from semiclassical dynamics are really non-linear features that arise from strong EM fields incident in the molecule. And yet, it is crucial to emphasize that Raman is a linear spectroscopy. From the KHD formula, the resonance Raman signal in the weak field regime scales as $|\mathbf{E}_S| \sim A_I$:

$$\left|\mathbf{E}_S\left(\omega_S = \frac{3}{4}\Omega\right)\right|^2 = A_I^2 \frac{\omega_S^2}{2\hbar^2 c^2}\frac{\mu^4}{\gamma^2}. \tag{31}$$

To address this feature, in Fig 2(b) we plot the Raman scattering intensity signal as obtained from Ehrenfest+R dynamics as a function of A_I. We show conclusively that the Ehrenfest+R signals is quadratic with respect to A_I, in agreement with the KHD formula.

V. CONCLUSIONS

In this work, we have generalized the Ehrenfest+R approach to treat a multi-level (more than two-level) system and we have demonstrated that such an approach recapitulates Raman scattering. In the context of a three-level system model, the proposed prescription of +R corrections can overcome the qualitative deficiencies of Ehrenfest dynamics and recover both (Stokes and anti-Stokes) resonant and off-resonant Raman scattering. In addition, a comparison with the quantum mechanical KHD formalism shows that Ehrenfest+R dynamics agrees quantitatively with resonant Raman scattering cross sections.

Given the promising results in this work, there are many further questions that need to be addressed. First, the proposed prescription is based on pairwise +R transitions without relative phases for rescaling fields. Do not the relative phases we have introduced also yield quantum fluctuations that one have ignored? Have we found the optimal semiclassical approach for quantum electrodynamics with more than two electronic states? Second, the data in this work was generated for a three level system in one dimension only, assuming that the polarization density has a simple Gaussian profile. Does our prescription work for a system with arbitrary polarization density in three dimensions ? Finally, the current setup includes one quantum subsystem only. How can we to treat the collective behavior of a set of molecular subsystems with strong electronic coupling? These questions will be investigated in the future.

ACKNOWLEDGMENT

This work is supported by AAA. We would like to thank BBB.

Appendix A: Scattering Cross section in a 1D space

Here we derive the scattering cross section for a 1D system within the KHD formalism.

Following Tannor's approach in Ref. 13, we take the rotating wave approximation (RWA) such that the electric field can be written as: $E_I e^{-i\omega_I t}$ for an incoming photon with amplitude E_I and frequency ω_I, and $E_S e^{i\omega_S t}$ for an outgoing photon with amplitude E_S and frequency ω_S. According to second order perturbation theory in Schrödinger picture, the expression for the second order wavefunction is

$$\begin{aligned}\left|\psi^{(2)}(t)\right\rangle = -\frac{1}{4\hbar^2}\int_{-\infty}^{t} dt_2 \int_{-\infty}^{t_2} dt_1 \\ e^{-\frac{i}{\hbar}\widehat{H}_0(t-t_2)}\left(\widehat{\mu}\cdot E_S e^{i\omega_S t_2}\right)\times \\ e^{-\frac{i}{\hbar}\widehat{H}_0(t_2-t_1)}\left(\widehat{\mu}\cdot E_I e^{-i\omega_I t_1}\right)\times \\ e^{-\frac{i}{\hbar}\widehat{H}_0 t_1}\left|\psi_i\right\rangle,\end{aligned} \tag{A1}$$

for the initial state of the system $|\psi_i\rangle$. Here $\widehat{H}_0$ is the unperturbed Hamiltonian of the electronic system and $\widehat{\mu}$ is the transition dipole operator.

Now we would like to extrapolate the change of the second order wavefunction to represent the number of the outgoing photons scattered per unit time. To do so, we evaluate the time derivative of the second-order wavefunction and insert a complete set of final states $|\psi_f\rangle$ to obtain:

$$\frac{\mathrm{d}}{\mathrm{d}t}\left\|\psi^{(2)}(t)\right\|^2 = \frac{2\pi E_S^2 E_I^2}{16\hbar^2}\sum_f \left|\alpha_{fi}(\omega_I)\right|^2 \delta(\omega_S - \Delta\omega) \tag{A2}$$

where the frequency-dependent polarizability is defined by

$$\alpha_{fi}(\omega_I) = \frac{i}{\hbar}\int_0^\infty d\tau \left\langle\psi_f\right| \widehat{\mu} e^{-\frac{i}{\hbar}\widehat{H}_0\tau}\widehat{\mu} e^{i(\omega_I+\omega_i)\tau}\left|\psi_i\right\rangle. \tag{A3}$$

Here $\Delta\omega = \omega_I + \omega_i - \omega_f$, and $\hbar\omega_i$ and $\hbar\omega_f$ are the energy levels of the initial and final states of the system. Then we apply the density of states for photons (but now for 1D system): $\rho(\omega_S) = \frac{L}{\pi c}$ and lead to

$$\frac{\mathrm{d}}{\mathrm{d}t}\left\|\psi^{(2)}(t)\right\|^2 = \frac{L}{8\hbar^2 c}E_S^2 E_I^2 \left|\alpha_{fi}(\omega_I)\right|^2. \tag{A4}$$

Lastly, we would like to eliminate the dependence of E_I and E_S in Eq. (A4) in order to express the scattering cross section in terms of photon frequencies. To do so ,we employ the Einstein relation of photons

$$\frac{E^2}{2} = \hbar\omega\frac{N}{L}. \tag{A5}$$

where $\frac{N}{L}$ is the photon density for a 1D system. Note that Eq. (A5) is valid for both incoming and scattered photons. For incoming photons, the incident field intensity can be written in terms of photon frequency and density:

$$E_I^2 = 2\hbar\omega_I\frac{N_I}{L}. \tag{A6}$$

For scattered photons, we consider spontaneous emission (i.e. $N_S = 1$) such that

$$E_S^2 = \frac{2\hbar\omega_S}{L}. \tag{A7}$$

With these relations, we rewrite Eq. (A4) as:

$$\frac{\mathrm{d}}{\mathrm{d}t}\left\|\psi^{(2)}(t)\right\|^2 = \frac{\omega_I\omega_S}{2c}\frac{N_I}{L}\left|\alpha_{fi}(\omega_I)\right|^2. \tag{A8}$$

Finally, we divide Eq. (A8) by the incident photon flux ($\frac{N_I c}{L}$) and obtain the Raman scattering cross section for a 1D system:

$$\sigma_{fi}^{\mathrm{1D}}(\omega_S,\omega_I) = \frac{\omega_I\omega_S}{2c^2}\left|\alpha_{fi}(\omega_I)\right|^2. \tag{A9}$$

REFERENCES

[1] K. A. Willets and R. P. Van Duyne, Annu Rev Phys Chem **58**, 267 (2007).
[2] P. L. Stiles, J. A. Dieringer, N. C. Shah, and R. P. Van Duyne, Annu Rev Anal Chem (Palo Alto Calif) **1**, 601 (2008).
[3] P. Vasa and C. Lienau, ACS Photonics **5**, 2 (2018).
[4] J. Gersten and A. Nitzan, The Journal of Chemical Physics **73**, 3023 (1980).
[5] D. A. Weitz, S. Garoff, J. I. Gersten, and A. Nitzan, The Journal of Chemical Physics **78**, 5324 (1983).
[6] S. M. Morton, D. W. Silverstein, and L. Jensen, Chem. Rev. **111**, 3962 (2011).
[7] X. Qian, X. Zhou, and S. Nie, J. Am. Chem. Soc. **130**, 14934 (2008).
[8] K. Qian, B. C. Sweeny, A. C. Johnston-Peck, W. Niu, J. O. Graham, J. S. DuChene, J. Qiu, Y.-C. Wang, M. H. Engelhard, D. Su, E. A. Stach, and W. D. Wei, Journal of the American Chemical Society **136**, 9842 (2014).
[9] T. Hartman, C. S. Wondergem, N. Kumar, A. van den Berg, and B. M. Weckhuysen, J. Phys. Chem. Lett. **7**, 1570 (2016).
[10] H. A. Kramers and W. Heisenberg, Z. Physik **31**, 681 (1925).
[11] P. A. M. Dirac, Proc. R. Soc. Lond. A **114**, 710 (1927).
[12] P. F. Bernath, *Spectra of Atoms and Molecules*, third edition ed. (Oxford University Press, Oxford, New York, 2015).
[13] D. J. Tannor, *Introduction to Quantum Mechanics: A Time-Dependent Perspective* (University Science Books, Sausalito, Calif, 2006).
[14] A. C. Albrecht, The Journal of Chemical Physics **34**, 1476 (1961).
[15] J. Tang and A. C. Albrecht, in *Raman Spectroscopy: Theory and Practice* (1970) pp. 33–68.
[16] D. A. Long, *The Raman Effect* (John Wiley & Sons, Ltd, Chichester, UK, 2002).
[17] S.-Y. Lee and E. J. Heller, The Journal of Chemical Physics **71**, 4777 (1979).
[18] E. J. Heller, R. Sundberg, and D. Tannor, J. Phys. Chem. **86**, 1822 (1982).
[19] D. J. Tannor and E. J. Heller, The Journal of Chemical Physics **77**, 202 (1982).
[20] E. J. Heller, Acc. Chem. Res. **14**, 368 (1981).
[21] J. Neugebauer and B. A. Hess, The Journal of Chemical Physics **120**, 11564 (2004).
[22] L. Jensen, J. Autschbach, and G. C. Schatz, The Journal of Chemical Physics **122**, 224115 (2005).
[23] L. Jensen, L. L. Zhao, J. Autschbach, and G. C. Schatz, The Journal of Chemical Physics **123**, 174110 (2005).
[24] D. Rappoport, S. Shim, and A. Aspuru-Guzik, J. Phys. Chem. Lett. **2**, 1254 (2011).
[25] M. Sukharev and A. Nitzan, J. Phys.: Condens. Matter **29**, 443003 (2017).
[26] S.-Y. Lee and E. J. Heller, The Journal of Chemical Physics **71**, 4777 (1979).
[27] P. W. Milonni, Physics Reports **25**, 1 (1976).
[28] T. E. Li, A. Nitzan, M. Sukharev, T. Martinez, H.-T. Chen, and J. E. Subotnik, Phys. Rev. A **97**, 032105 (2018).
[29] H.-T. Chen, T. E. Li, M. Sukharev, A. Nitzan, and J. E. Subotnik, arXiv:1806.04662 (2018).
[30] S. Mukamel, *Principles of Nonlinear Optics and Spectroscopy* (Oxford University Press, 1999).
[31] P. A. M. Dirac, Proc. R. Soc. Lond. A **114**, 243 (1927).